



with different orientations of a spiral phase filter [7]. Qiu *et al.* [8] combined a nonlinear filter with second harmonic generation in the Fourier domain to achieve a visible edge enhancement with invisible illumination. Song *et al.* [13] presented an experimental configuration to accomplish non-local SPC imaging with classical incoherent thermal light illumination. Liu *et al.* [11] presented a single-pixel SPC imaging technique that could benefit low-cost systems. Liu *et al.* [14] developed a real-time quantum edge enhanced imaging method by combining SPC technique with heralded single-photon imaging. Zhu *et al.* [15] proposed a method for inversely designing the spatial filter to achieve high-resolution images. In addition, some physical filters, such as the Laguerre–Gaussian spatial filter [16] and Airy spiral phase filter [17] have been presented to achieve high contrast edge enhancement.

Generally speaking, edge enhancement is usually performed in free space. These methods may meet challenging when the system involves complex media, such as white paint, thick biological tissues, and multimode fiber. In this situation, light propagates inside complex media and undergoes multiple scattering, thus optical information is scrambled [18, 19]. Therefore, existing SPC imaging technique encounters challenging as all other biomedical optical imaging techniques. In order to image through complex media, many methods such as optical phase conjugation [20, 21], transmission matrix (TM) method [18, 22], Speckle-Correlation Scattering Matrix method [23], and speckle correlation [19] have been presented. To achieve edge detection through complex media, Zihao Li and his colleagues [24] presented a digital optical phase conjugation setup to achieve edge enhancement through scattering media. Thanks to the existence of the transition status for edges of the object, an effective two-step procedure has been successfully utilized for detecting the edges of amplitude objects beyond high scattering. However, to the best of our knowledge, the extraction of the boundary information of invisible phase objects through complex media has not been demonstrated yet.

To address this issue, we present a TM-based operator that enables SPC imaging through complex media. We build this new operator by numerically applying a spiral phase filtering in a virtual Fourier plane of the input modes of the experimentally calibrated TM. Experimentally, the proposed technique is first demonstrated by imaging two digital objects. The edge enhanced images of both amplitude and phase objects are obtained, and the correlation coefficient between the reconstructed edge enhanced image and the theoretical edge enhanced image is calculated to be  $\sim 0.9$ . Further, we find that the correlation coefficient increases with the ratio between the numbers of output modes and input modes. In addition, we apply this technique to image two real objects, including amplitude and phase objects. Isotropic edge

contrast enhancement is clearly achieved in all the experiments. We believe this work will pave the way for edge detection of objects through the complex media, for example, the invisible phase biological cells in deep tissues.

## 2 Principle

Figure 1 illustrates the principle. Our method achieves spiral phase contrast imaging based on the transmission matrix of the complex medium, which is denoted  $T$ . Its complex coefficients  $t_{X'X}$  connect the optical field at the output plane and the input plane which correspond to camera pixel coordinates  $X'(x', y')$  and object coordinates  $X(x, y)$  by

$$E_{X'}^{out} = \sum_X (t_{X'X} E_X^{in}). \quad (1)$$

Here, the input plane and output plane are divided into  $N$  input modes and  $M$  output modes, respectively. The elements  $t_{X'X}$  can be calibrated by using phase shifting method [25]. Due to multiple scattering, the wavefront of an object  $E_X^{object}$  illuminated by a coherent light source is scrambled when passing through complex medium, generating speckle pattern at the output plane. If the field of speckle pattern  $E_{X'}^{out}$  is measured, we can retrieve the object image by performing the inverse of  $T$  [18]:

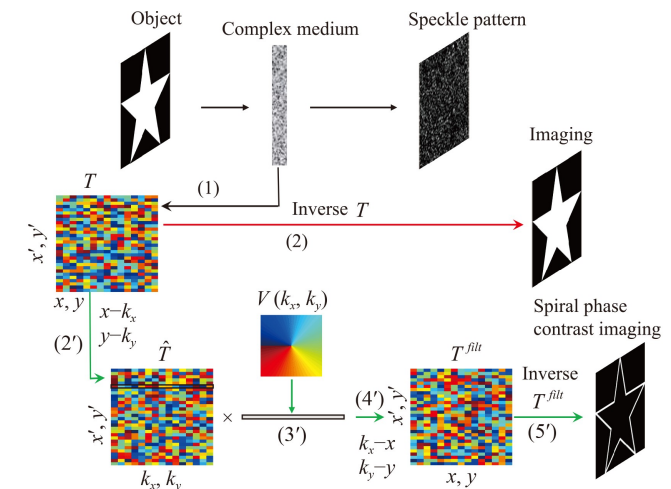


**Fig. 1** Principle of transmission matrix based spiral phase contrast imaging through complex medium. (1) Operation of acquiring transmission matrix  $T$  of the complex medium. (2) Imaging through complex medium by use of the inverse  $T$ . (2') Operation of obtaining  $\hat{T}$  by performing a two-dimensional spatial Fourier transform on  $T$  of every input field. (3')  $\hat{T}$  is filtered by a spiral phase function  $V$ . (4') Return to the spatial domain by taking an inverse Fourier transform on the term of  $\hat{T} \times V$ . (5') Spiral phase contrast imaging through complex medium by applying the inverse  $T^{filt}$ .

$$E_X^{object} = T^\dagger E_{X'}^{out}, \quad (2)$$

where  $T^\dagger$  represents the inverse matrix of  $T$ . In general, it is the pseudoinverse matrix of  $T$  when the ratio  $\gamma = M/N$  is arbitrary. Here, we assume  $\gamma > 1$ ,  $T^\dagger = (T^* \times T)^{-1} \times T^*$ , where  $T^*$  is the transpose conjugate matrix of  $T$ . In a physical picture, TM describes the relationship between the output field and the input field in the system that involves complex media, compared to free space that uses point spread function (PSF) to describe the pulse response of the imaging system. To achieve spiral phase contrast imaging, a filtered PSF is usually constructed to obtain the edge enhanced image in free space. In our case, we present a TM-based operator to play the similar role as the filtered PSF in free space but consider the scattering effects at the same time.

We first perform a Fourier transform on  $T$  of every input field, that is  $\hat{t}_{X'K} = \mathfrak{F}(t_{X'X})$ , where  $K = (k_x, k_y)$  is the wave vector associated with  $X$ . And the obtained  $\hat{T}$  is the corresponding TM in a Fourier plane of the input mode plane. In order to implement a radial Hilbert transform for the input field, a vortex phase (topological charge  $l = 1$ ) is used in the process of reconstructing the image, which plays as a spatial filter at the virtual Fourier plane of the input modes of the experimentally calibrated TM, and can be described as

$$V(k_x, k_y) = \exp(j\phi(k_x, k_y)), \quad (3)$$

where  $\phi(k_x, k_y) = \arctan(k_y/k_x)$ . Thus a new numerically filtered coefficient in the Fourier domain can be obtained by

$$\hat{t}_{X'K}^{filt} = \hat{t}_{X'K} \times V(k_x, k_y). \quad (4)$$

Then we go back to the spatial domain  $XX$  by taking the inverse Fourier transform of  $\hat{t}_{X'K}^{filt}$ :

$$t_{X'X}^{filt} = \mathfrak{F}^{-1}(\hat{t}_{X'K}^{filt}). \quad (5)$$

With the above operations, the resulting  $T^{filt}$  is equivalent to taking a convolution between  $T$  and the Fourier transform of  $V(k_x, k_y)$  in the input mode plane. Thus in the process of retrieving the image from the output speckle field,  $T^{filt}$  can be seemed as characterizing the propagation of light in a complex system whose PSF is Fourier spectrum of the vortex filter. Therefore, when

$T^{filt}$  is used to instead of  $T$  to perform the operation of inverse TM, i.e.,

$$E_{X'}^{oee} = T^{filt+} E_{X'}^{out}. \quad (6)$$

The obtained  $E_{X'}^{oee}$  is the complex field of object with edge enhancement.

### 3 Experimental setup

In order to validate the theoretical proposal, we perform experiment of spiral phase imaging through complex media for both digital objects and real objects. The schematic of experimental setup is shown in Fig. 2. To achieve a fast wavefront shaping [26, 27], a DMD (Vialux V-7001) which can switch at a rate of 22.727 kHz is employed as the spatial light modulator. A laser beam with the wavelength of 532 nm is expanded and steered to fully illuminate the DMD. Then with the assistance of a  $4f$  configuration and a spatial filter, the DMD enables to modulate the complex amplitude of light in its first-diffraction-order beam in terms of the Lee method [28]. To image the real object, a plane wave modulated by DMD is used to illuminate the object which is located at the focal plane of L4. Then the transmitted light illuminates on a ZnO scattering layer via an objective OBJ1 (10X, NA = 0.25). Here, a ZnO scattering layer with the thickness of about 280  $\mu\text{m}$  is fabricated by depositing the ZnO powder on a 170  $\mu\text{m}$  thick cover glass, is used as the complex medium. The transmittance of ZnO scattering layer is about 6%. Then the resultant speckle field is collected by OBJ2 (20X, NA = 0.4) and imaged by a CMOS camera (D752, PixeLINK) with a tube lens L5. To achieve spiral phase contrast imaging, the TM and the resultant speckle field of the objects should be measured first. The phase shifting method [25] is applied for the measurement, with a plane wave reference introduced. In the calibration of TM,  $N = 32 \times 32$  input segments on the DMD and  $M = 480 \times 480$  pixels on camera are respectively used as the input and output modes.

### 4 Results

To demonstrate our presented scheme for edge detection

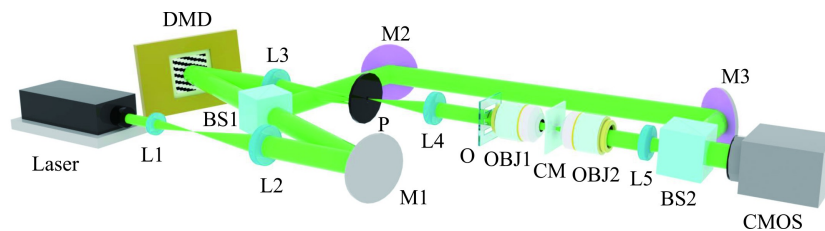


**Fig. 2** Experimental setup. L: Lens; M: Mirror; BS: Beam splitter; DMD: Digital micro-mirror device; P: Pinhole; O: Object; OBJ: Objective; CM: Complex medium; CMOS: Complementary metal-oxide-semiconductor camera.

through complex media, we first image a digital amplitude object of a star and a digital phase object of a moon. The two binary objects are generated by the DMD. The intensity distribution of the star and phase distribution of the moon are presented in Figs. 3(a) and (b), respectively. When the field carrying the information of objects is transmitted through the ZnO scattering layer, we obtain intensity speckle patterns at the camera plane, which are respectively presented in Figs. 3(c) and (d). For a comparison, we first reconstruct the images by performing inverse  $T$  and the corresponding results are presented at the inset of Figs. 3(c) and (d). Then we obtain the edge enhanced images [see Figs. 3(e) and (f)] by adopting TM-based spiral phase contrast imaging technique. As we can see, the boundary information of the two objects are successfully extracted. To quantify the ability of spiral phase imaging, the correlation coefficients between the objects theoretically filtered by the spiral phase in a  $4f$  configuration and our results are calculated. For the two digital objects imaged, the correlation coefficients are 0.8838 and 0.9221. For further

examination, two intensity profiles along the white dashed lines through the two edge enhanced images are presented in Figs. 3(g) and (h). As we can see, the locations of the recovered edges are in good agreement with the theoretically calculated locations. However, the edge enhanced image is not perfect due to the reconstruction noise. Furthermore, we find that the reconstruction noise can be lowered by increasing the ratio ( $\gamma = M/N$ ) between the numbers of output modes and input modes. The quantitative analysis is presented in Fig. 3(i). As the curve shows, the fidelity of the reconstructed edge enhanced images is improved with the increasing of  $\gamma$ , and correlation coefficient reaches 80% when  $\gamma$  is about 60. In theory, the eigenmodes of the scattering system and their singular values can be obtained based on the singular value decomposition of the TM. The singular values are proportional to the amplitude transmitted through each channel of the system. According to random matrix theory, the minimum singular value increases with  $\gamma$  [29]. The TM calibration process could be insensitive to the experimental noise when the energy

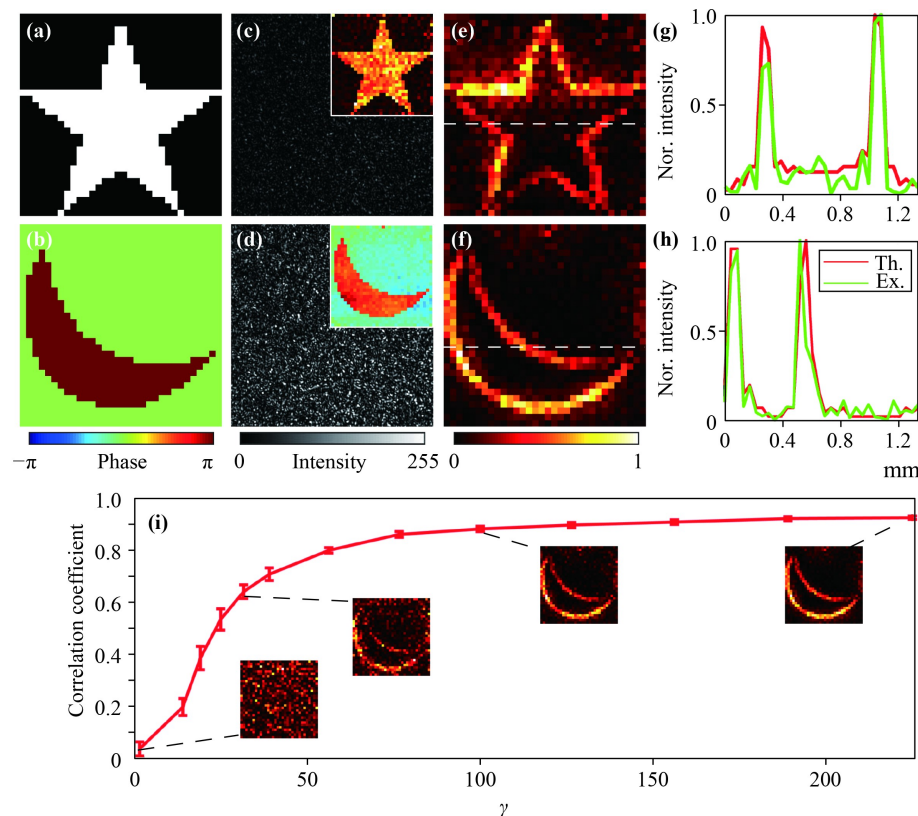


**Fig. 3** Edge detection of digital amplitude and phase objects by applying TM-based spiral phase contrast imaging technique. (a) The intensity distribution of the amplitude object of a star. (b) The phase distribution of the phase object of a moon. (c, d) Intensity speckle patterns at the output plane when the field of object transports through the ZnO scattering layer. The inset are the reconstructed images with the conventional inverse  $T$  operation. (e, f) The edge enhanced images with our presented technique. (g, h) The intensity profiles along the white dashed lines in (e, f), respectively. The green and red lines are the experimental data and theoretical data. (i) Correlation coefficient between the recovered edge enhanced images and the images digitally filtered by a spiral phase as a function of  $\gamma$  which is the ratio between the numbers of output modes and input modes.

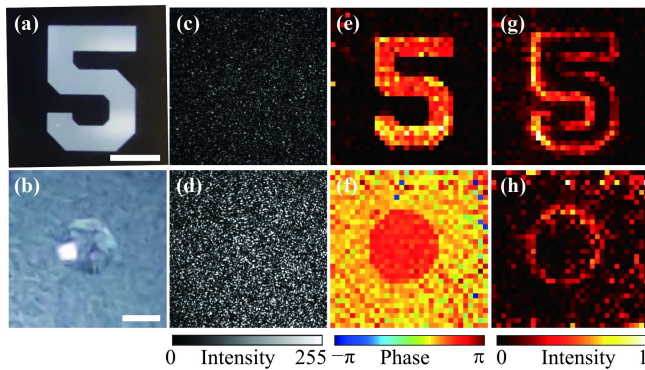


**Fig. 4** Edge detection of real amplitude and phase objects by applying TM-based spiral phase contrast imaging technique. (a) A binary amplitude object of number “5”. (b) A phase object formed by an oil droplet on a cover glass. (c, d) The recorded intensity speckle patterns at the camera plane. (e, f) The corresponding reconstructed images with the conventional inverse  $T$  operation. (g, h) The corresponding edge enhanced images obtained with our presented technique. Scale bar, 1 mm.

transported by the most inefficient channel reaches the noise level. As a result, reconstruction noise can be lowered by increasing  $\gamma$ . Note that  $N$  is the number of the input modes, and thus it directly determines the resolution of the reconstructed image. Therefore, if  $M$  keeps unchanged and  $N$  is decreased to enlarge  $\gamma$ , the image resolution is decreased even though the reconstruction noise is lowered. In this case, the reconstruction fidelity characterizing the correlation coefficient between the reconstructed image and the original input object is hard to evaluate. Thus it is a better choice to enlarge  $\gamma$  by increasing  $M$ .

Apart from imaging the digital objects, we further apply our technique to image real objects including both amplitude and phase objects. An amplitude object of number “5” (USAF1951, Thorlabs) [Fig. 4(a)] and an oil droplet on a cover glass [Fig. 4(b)] are placed on the focal plane of L4 and employed as amplitude and phase objects, respectively. A plane wave modulated by DMD is employed to illuminate the objects. The original speckle patterns recorded by the camera are respectively represented in Figs. 4(c) and (d). For a comparison, the images of the objects obtained by the inverse  $T$  operation [Figs. 4(e) and (f)] and their edge enhanced images obtained by applying TM-based spiral phase contrast imaging technique [Figs. 4(g) and (h)] are presented. As we can see, both of their edges have been clearly reconstructed with our presented scheme. Note that the defocused image may be caused by the slight deviation of the object’s position in terms of the exact input plane.

## 5 Conclusions

In summary, we have proposed a TM-based spiral phase

contrast imaging technique for edge detection of both amplitude and phase objects through complex media. By combining the TM based imaging through the complex media with spiral phase filtering, this technique allows us to directly reconstruct the edge enhanced images through the complex media. Experimentally, we have demonstrated the strength of this technique by imaging both digital and real objects. The isotropic edge contrast enhancement is clearly achieved in experiments. In particular, we demonstrate that the fidelity of the reconstructed edge enhanced images can be improved by increasing the ratio between output modes and input modes. The proposed method is expected to open up possibilities for detection of invisible phase objects through complex media.

**Acknowledgements** This work was supported by the National Key Research and Development Program of China (No. 2019YFA0705000), the National Natural Science Foundation of China (NSFC) (Nos. 12004219, 120742251, 2192254, 91750201, and 11974218), the Innovation Group of Jinan (No. 2018GXRC010), and the Local Science and Technology Development Project of the Central Government (No. YDZX20203700001766).

## References

1. D. Mawet, E. Serabyn, J. K. Wallace, and L. Pueyo, Improved high-contrast imaging with on-axis telescopes using a multistage vortex coronagraph, *Opt. Lett.* 36(8), 1506 (2011)
2. A. Jesacher, S. Fürhapter, S. Bernet, and M. Ritsch-Marte, Shadow effects in spiral phase contrast microscopy, *Phys. Rev. Lett.* 94(23), 233902 (2005)
3. F. Qadir, M. Peer, and K. Khan, Efficient edge detection methods for diagnosis of lung cancer based on two-dimensional cellular automata, *Adv. Appl. Sci. Res.* 3(4), 2050 (2012)
4. P. Nisthula and R. Yadhu, A novel method to detect bone cancer using image fusion and edge detection, *Int. J. Eng. Comp. Sci.* 2(6), 2012 (2013)
5. T. Zhu, Y. Zhou, Y. Lou, H. Ye, M. Qiu, Z. Ruan, and S. Fan, Plasmonic computing of spatial differentiation, *Nat. Commun.* 8(1), 15391 (2017)
6. S. Fürhapter, A. Jesacher, S. Bernet, and M. Ritsch-Marte, Spiral phase contrast imaging in microscopy, *Opt. Express* 13(3), 689 (2005)
7. S. Bernet, A. Jesacher, S. Fürhapter, C. Maurer, and M. Ritsch-Marte, Quantitative imaging of complex samples by spiral phase contrast microscopy, *Opt. Express* 14(9), 3792 (2006)
8. X. Qiu, F. Li, W. Zhang, Z. Zhu, and L. Chen, Spiral phase contrast imaging in nonlinear optics: Seeing phase objects using invisible illumination, *Optica* 5(2), 208 (2018)
9. C. Zhou, G. Wang, H. Huang, L. Song, and K. Xue, Edge detection based on joint iteration ghost imaging, *Opt. Express* 27(19), 27295 (2019)
10. H. Ren, S. Zhao, and J. Gruska, Edge detection based

- on single-pixel imaging, *Opt. Express* 26(5), 5501 (2018)
11. Y. Liu, P. Yu, X. Hu, Z. Wang, Y. Li, and L. Gong, Single-pixel spiral phase contrast imaging, *Opt. Lett.* 45(14), 4028 (2020)
  12. J. A. Davis, D. E. McNamara, D. M. Cottrell, and J. Campos, Image processing with the radial Hilbert transform: Theory and experiments, *Opt. Lett.* 25(2), 99 (2000)
  13. H. Song, Y. Zhang, Y. Ren, Z. Yuan, D. Zhao, Z. Zheng, and L. Gao, Non-local edge enhanced imaging with incoherent thermal light, *Appl. Phys. Lett.* 116(17), 174001 (2020)
  14. S. K. Liu, Y. H. Li, S. L. Liu, Z. Y. Zhou, Y. Li, C. Yang, G. C. Guo, and B. S. Shi, Real-time quantum edge enhanced imaging, *Opt. Express* 28(24), 35415 (2020)
  15. X. Zhu, H. Yao, J. Yu, G. Gbur, F. Wang, Y. Chen, and Y. Cai, Inverse design of a spatial filter in edge enhanced imaging, *Opt. Lett.* 45(9), 2542 (2020)
  16. C. S. Guo, Y. J. Han, J. B. Xu, and J. Ding, Radial Hilbert transform with Laguerre–Gaussian spatial filters, *Opt. Lett.* 31(10), 1394 (2006)
  17. Y. Zhou, S. Feng, S. Nie, J. Ma, and C. Yuan, Image edge enhancement using Airy spiral phase filter, *Opt. Express* 24(22), 25258 (2016)
  18. S. Popoff, G. Lerosey, M. Fink, A. C. Boccara, and S. Gigan, Image transmission through an opaque material, *Nat. Commun.* 1(1), 81 (2010)
  19. J. Bertolotti, E. G. van Putten, C. Blum, A. Lagendijk, W. L. Vos, and A. P. Mosk, Non-invasive imaging through opaque scattering layers, *Nature* 491(7423), 232 (2012)
  20. Z. Yaqoob, D. Psaltis, M. S. Feld, and C. Yang, Optical phase conjugation for turbidity suppression in biological samples, *Nat. Photonics* 2(2), 110 (2008)
  21. J. Yang, Y. Shen, Y. Liu, A. S. Hemphill, and L. V. Wang, Focusing light through scattering media by polarization modulation based generalized digital optical phase conjugation, *Appl. Phys. Lett.* 111(20), 201108 (2017)
  22. Y. Choi, C. Yoon, M. Kim, T. D. Yang, C. Fang-Yen, R. R. Dasari, K. J. Lee, and W. Choi, Scanner-free and wide-field endoscopic imaging by using a single multimode optical fiber, *Phys. Rev. Lett.* 109(20), 203901 (2012)
  23. Y. Baek, K. Lee, and Y. Park, High-resolution holographic microscopy exploiting speckle-correlation scattering matrix, *Phys. Rev. Appl.* 10(2), 024053 (2018)
  24. Z. Li, Z. Yu, H. Hui, H. Li, T. Zhong, H. Liu, and P. Lai, Edge enhancement through scattering media enabled by optical wavefront shaping, *Photon. Res.* 8(6), 954 (2020)
  25. S. Popoff, G. Lerosey, R. Carminati, M. Fink, A. Boccara, and S. Gigan, Measuring the transmission matrix in optics: An approach to the study and control of light propagation in disordered media, *Phys. Rev. Lett.* 104(10), 100601 (2010)
  26. Q. Zhao, P. P. Yu, Y. F. Liu, Z. Q. Wang, Y. M. Li, and L. Gong, Light field imaging through a single multimode fiber for OAM-multiplexed data transmission, *Appl. Phys. Lett.* 116(18), 181101 (2020)
  27. L. Gong, Q. Zhao, H. Zhang, X. Y. Hu, K. Huang, J. M. Yang, and Y. M. Li, Optical orbital-angular-momentum-multiplexed data transmission under high scattering, *Light Sci. Appl.* 8(1), 27 (2019)
  28. X. Hu, Q. Zhao, P. Yu, X. Li, Z. Wang, Y. Li, and L. Gong, Dynamic shaping of orbital-angular-momentum beams for information encoding, *Opt. Express* 26(2), 1796 (2018)
  29. R. Sprik, A. Tourin, J. de Rosny, and M. Fink, Eigenvalue distributions of correlated multichannel transfer matrices in strongly scattering systems, *Phys. Rev. B* 78(1), 012202 (2008)